

Hole Mobility and its enhancement with Strain for technologically relevant III-V semiconductors

Aneesh Nainani, Donghyun Kim, Tejas Krishnamohan and Krishna Saraswat

Center for Integrated Systems, Department of Electrical Engineering, Stanford University, CA 94305 USA

Phone: 650-521-2623, Email: nainani@stanford.edu

Background: III-V semiconductors are one of the most promising device candidates for future high-speed, low-power logic applications due to their high electron mobility. Recently, high performance III-V n-FETs have been demonstrated [1]. However, for CMOS logic, there is a significant challenge of identifying high mobility III-V p-FET candidates [2]. Strain in silicon initially in Si layers on relaxed SiGe buffer layers, later from SiGe spacers / spacer caps has been successful in significantly enhancing the pMOS performance and is now employed ubiquitously in the industry. Use of strain to reduce hole effective masses by splitting the heavy-hole (*hh*) and light-hole (*lh*) valence bands was first demonstrated in *p*-channel InGaAs/ (Al)GaAs [3-4]. More recently, the technique has been applied to strained InSb [5], GaSb [6] and InGaSb [7] based channels for improving hole nobility (μ_h). Given the many choices available for materials, stoichiometry, strain, channel orientation, a modeling effort is necessary to evaluate different options and narrow down the choice for experimentation.

Introduction: In this paper we use 8 band k.p approach to model the bandstructure for technologically relevant Arsenic (As) and Antimony (Sb) based III-V compounds. 8x8 Hamiltonian with spin orbit coupling [8] is used to evaluate strain. Parameters used for simulation are calibrated against bulk bandstructure obtained using non-local empirical pseudopotential method (EPM) with and without strain. A self consistent method is used to calculate the valence subband structure [9] (Figure1). (100), (110) and (111) wafer orientations with different strain configurations are evaluated to identify the optimum configuration.

Band Structure and Calibration: Figure 1 shows the band structure for InSb calculated using 6/8 band k.p & EPM methods. 8-band model matches the EPM results better than 6-band k.p, especially for the split-off subband and as we move away from the Γ point due to significant coupling of the conduction band with valence bands. Figure 2 plots the calculated Density of States (DOS) & DOS effective mass (m_{DOS}) for *lh/hh* bands in InSb and GaAs. Figure 3 plots the isoenergy surfaces of the upper VB at 2, 25 and 50 meV. We see that in III-V's the valence-band energy surfaces remain relatively isotropic as compared to silicon where the valence-band becomes increasingly anisotropic with increasing energy.

Tertiary III-V's & Strain: Bandstructures of $In_xGa_{1-x}As$ and $In_xGa_{1-x}Sb$ are calculated using the band parameters of binary end points (interpolated using bowdin theory [10]). Effect of strain is analyzed by using the 8x8 Hamiltonian of [8]. Figure 4 plots the band energies & shifts with uniaxial/biaxial tensile & compressive strain in $In_xGa_{1-x}As$ as a function of *x* using EPM. Band shifts from k.p are matched with EPM results. Figure 5 shows the isoenergy surfaces for the top valence band of GaAs with biaxial and uniaxial-[110] compression. For biaxial stress, the energy surface is an

ellipsoid with the energy contours in the *x-y* plane being circles (Figure 5(a)), the band is *lh*-like in the plane of the stress & *hh*-like out-of-plane. Under uniaxial compression (along [110]), the energy contour for the top band in the *x-y* plane is an ellipse with the major axis along [-110] and the minor axis along [110]. Though qualitatively the strain behavior in *p*-channel III-Vs is similar to group-IV elements, the prime differences arise from: (a) initial isotropy of the valence bands in III-V as compared to Si/Ge, (b) lower modulus of elasticity resulting in more strain for the same amount of stress in III-V's as compared to Si/Ge (Table. 1) and (c) additional effect due to increased mixing with Conduction band specially for III-V's with low-bandgap.

Hole Mobility (μ_h): Table. 1 lists the low field mobility for binary III-V's. We use the approach of [11] accounting for acoustic/optical deformation potential, alloy and polar scattering mechanisms to calculate the hole mobility. Deformation potentials and most of the parameters needed for μ_h calculations are taken from [10,12]. Unlike for electrons in III-V where polar scattering is the dominant scattering mechanism (non polar optical phonons do not interact due to *s*-like spherical symmetry of conduction band in III-V's [12])) both deformation potential and polar scattering mechanisms are important for μ_h calculations. In Table.1 we observe that varying group III element while keeping the group V element same (i.e. InAs \rightarrow GaAs) μ_h does not change appreciably while a large change is observed when the group V element is varied (i.e. InP \rightarrow InAs \rightarrow InSb). This is a consequence of the fact that the valence bands of III-V mostly derive from the *p*-orbitals of the anion [13]. Figure 6 plots the low field μ_h of $In_xGa_{1-x}As$ and $In_xGa_{1-x}Sb$ (Sheet Charge (N_S) = $10^{12}/cm^2$). We observe that the μ_h for the tertiary III-Vs roughly stay between those of the binary end points. Sb's have significantly higher mobilities than As's. Note that at higher fields the mobility of the tertiaries is expected to be less than that of the end point binaries due to increased alloy scattering.

Surface Orientation: Figure 7 plots the effect of surface orientation & channel direction on μ_h of As/Sb binaries. Three standard surface orientations (001), (110), (111) and all possible channel directions are considered. We observe that (111) orientation is marginally better than the others. While (100) orientation is isotropic along all channel directions (similar to Si/Ge [14]), (110)/(111) surfaces have slight anisotropy (though much less compared to (110) in Si/Ge [14]).

Mobility Enhancement with Strain: Next we study the effect of biaxial & uniaxial strain on μ_h enhancement in these binaries for the three surface orientations mentioned above and all channel directions. As the μ_h enhancement for the tertiary lies in between the corresponding binaries). Figure 8 shows plots the μ_h enhancement with respect to the unstrained case (for uniaxial case the strain is always applied along the channel direction). In all cases

compression is better than tension for μ_h enhancement. For biaxial case: enhancement in (100) is isotropic, while in (110)/(111) it depends on the direction of the channel; maximum enhancement with 2% biaxial strain is 2.3X. Much higher μ_h enhancement is achieved with same % of uniaxial strain (4.3X with 2% uniaxial compression - best case Figure8) also the enhancement is highly anisotropic. Also note that ~ 2 times lower stress is required to produce the same amount of strain in InSb/GaSb due to their lower elasticity constants as compared to Si. Finally trends from simulation are compared with experimental data in Figure 9, and a good match is obtained.

Conclusion: A comprehensive analysis is performed for μ_h enhancement in III-V's with strain. (In/Ga/In_xGa_{1-x})Sb's due to their higher μ_h which gets significantly enhanced with strain (Figure9) appear promising candidates for III-V p-FETs.

Acknowledgement: The authors are grateful to Intel Corp. for providing support for this work.

Reference

[1] B. R. Bennett et. al. Solid-State Electron. 49,1875
 [2] P. P. Ruden et. al, IEEE Transactions on Electron Devices, 36, 2371.
 [3] G. C. Osbourn, Superlattices and Microstructures 1, 223.
 [4] M. Jaffe et. al., Applied Physics Letters, 54, 2345.
 [5] M. Radasavljevic, International Electron Device Meeting 2008, pp. 727.
 [6] B. R. Bennett et. al. Journal of Crystal Growth, 311, 47.
 [7] B. R. Bennett et al, Applied Physics Letters, 91,042104.
 [8] T.B. Bahder et. al., Physical Review B, 41, 11992.
 [9] Y. Zhang et. al., Journal of Computational Electronics, submitted
 [10] I. Vurgaftman et. al., Journal of Applied Physics, 89, 5815
 [11] MV Fischetti et. al., Journal of Applied Physics, 94, 1079.
 [12] J. D. Wiley, Semiconductor and Semimetals, 10, 91
 [13] G. Bastard, Wave Mechanics Applied to Semiconductor Hetrostructures, 1988
 [14] T. Krishnamohan et. al, International Electron Device Meeting 2008, pp. 899

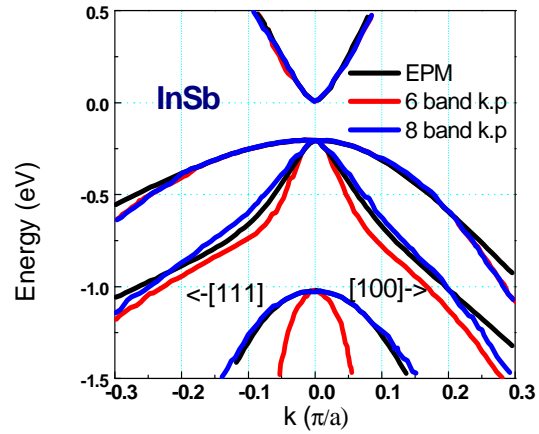


Fig.1 Bandstructure of InSb using 6- band / 8-band k.p & EMP methods.

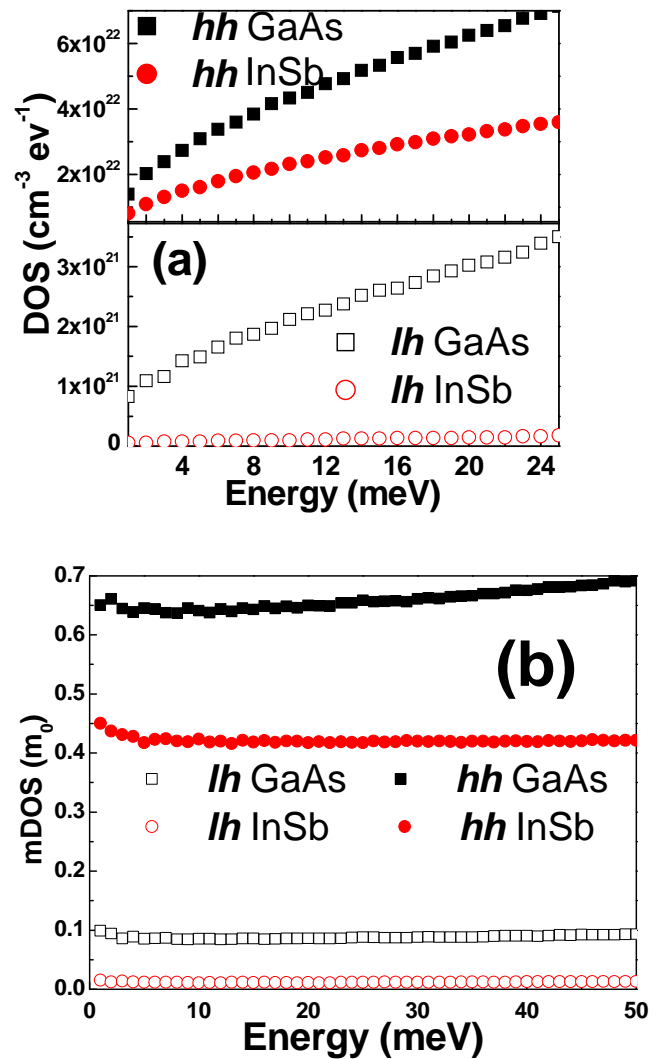


Fig.2 (a) Density of State (DOS) & (b) Density of state mass (mDOS) for lh & hh bands in GaAs & InSb.

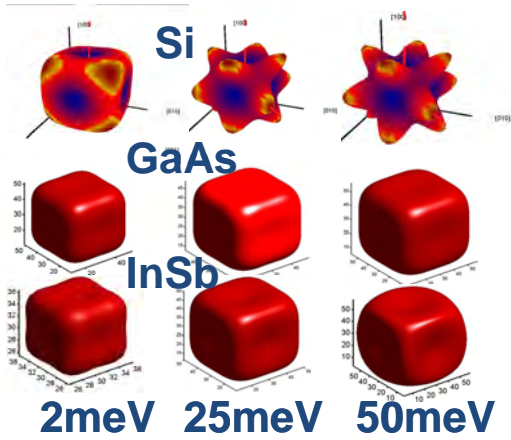


Fig.3 Isoenergy surfaces at 2/25/50meV for the upper VB in Si/InSb/GaAs. Si becomes increasingly anisotropic with energy while III-V's maintain anisotropy.

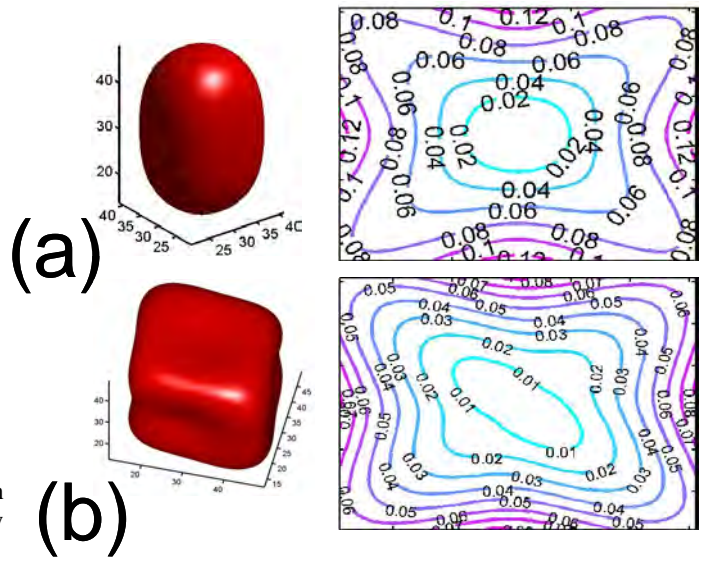


Fig.5: Isoenergy surface of upper VB in GaAs under (a) biaxial (b) uniaxial compression.

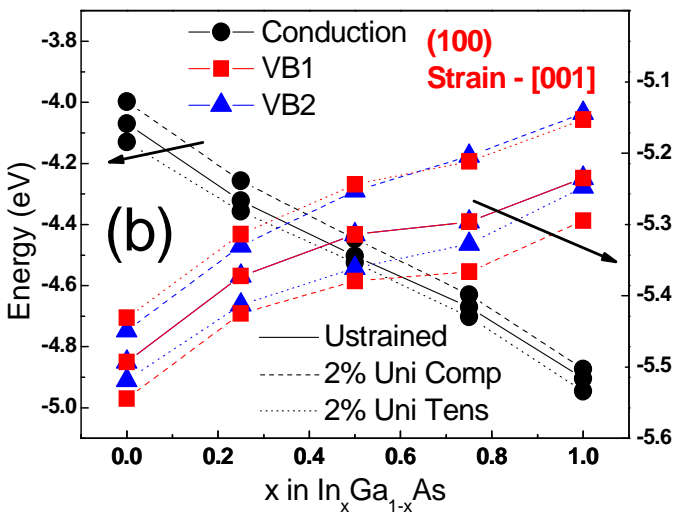
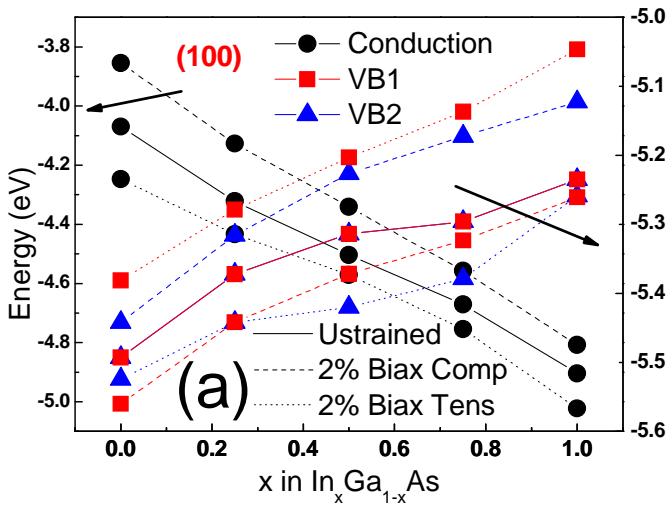


Fig.4 Bandshifts in $In_xGa_{1-x}As$ with (a) Biaxial (b) Uniaxial Compressive/Tensile Strain.

Table 1 : Low Field mobility values in III-V. Note that III-V's (Sb's in particular) have lower elasticity constants than Si making application of process strain easier.

	E_g (eV)	m_{lh}	m_{hh}	Bulk Mod. (dyne/cm ²)	μ_h (cm ² /Vs)
GaP	2.26	0.14 m_0	0.79 m_0	8.8x10 ¹¹	150
GaAs	1.42	0.08 m_0	0.51 m_0	7.1x10 ¹¹	400
GaSb	0.72	0.05 m_0	0.4 m_0	5.63x10 ¹¹	800
InP	1.34	0.09 m_0	0.6 m_0	8.8x10 ¹¹	200
InAs	0.35	0.03 m_0	0.41 m_0	5.8x10 ¹¹	450
InSb	0.17	0.02 m_0	0.43 m_0	4.7x10 ¹¹	850
Si	1.1	0.17 m_0	0.49 m_0	9.9x10 ¹¹	450

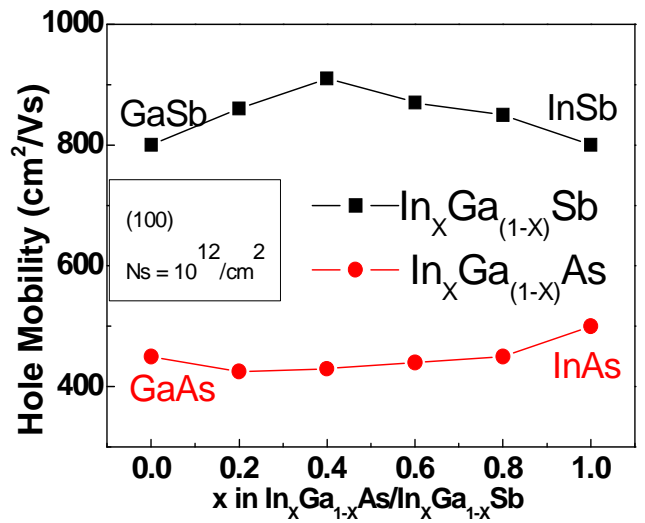


Fig.6. Hole Mobility for $In_xGa_{1-x}Sb$ and $In_xGa_{1-x}As$. We observe that Sb's have higher hole mobilities than As's

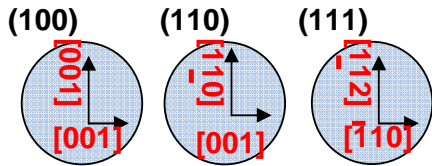
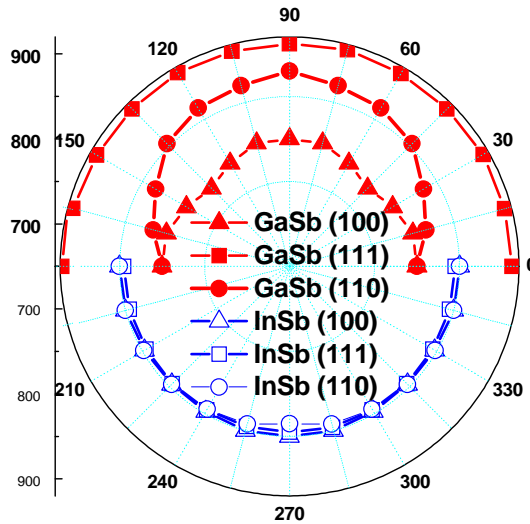
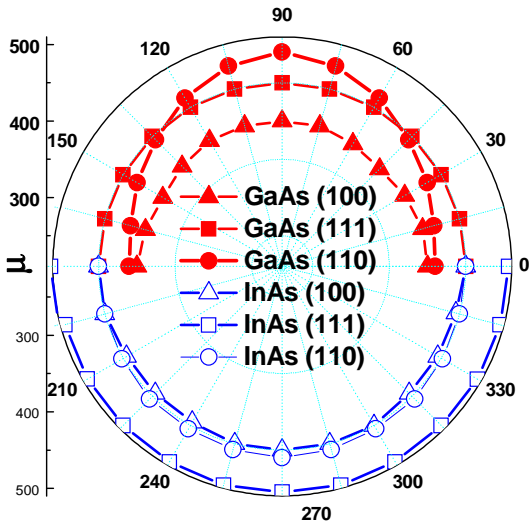


Fig.7.(above) Effect of surface orientation & channel direction on hole mobility is studied in GaAs/InAs/GaSb/Insb ($N_s = 10^{12}/\text{cm}^2, T=300\text{K}$), for the 3 common surface orientation and all possible channel directions.

Fig 9. (below) Modeling results for biaxial strain on (100) are compared with experimental data on strained heterostructures. $N_s \sim 10^{12}/\text{cm}^2$ for most data points while T_{CHANNEL} is different.

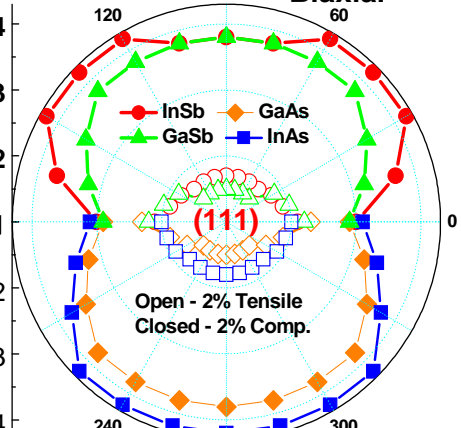
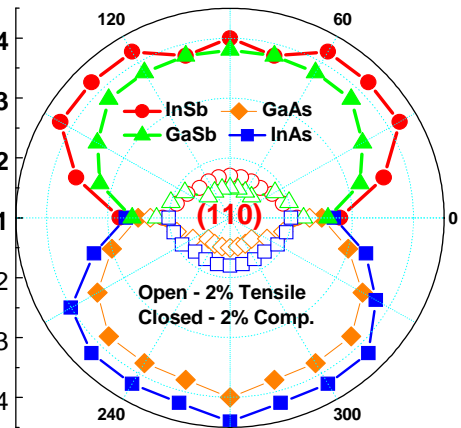
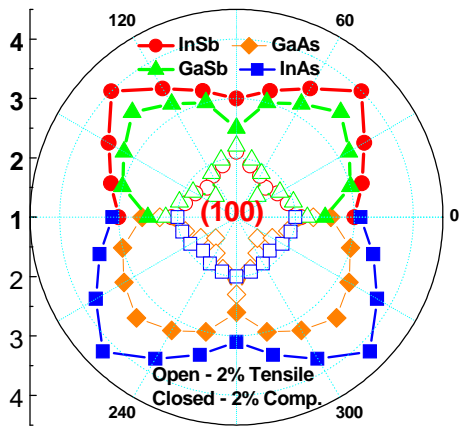
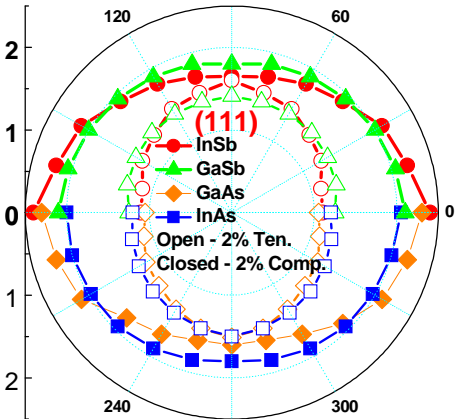
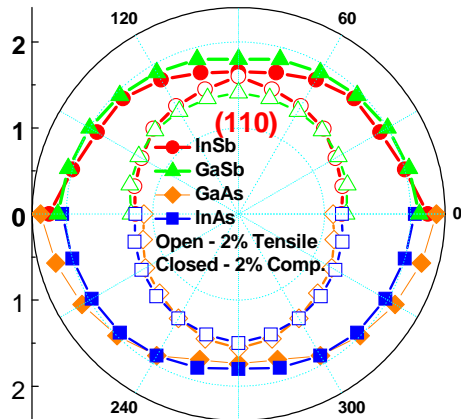
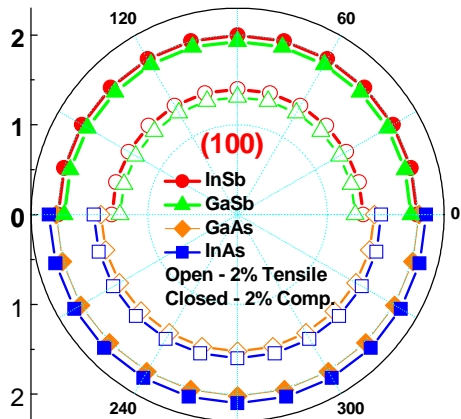
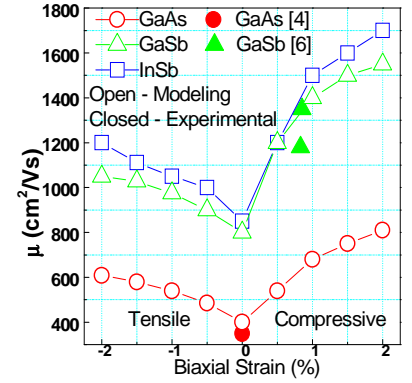


Fig 8. Enhancement of mobility with respect to the unstrained case (Fig.7) with biaxial (top) uniaxial (bottom) strain. Enhancement with compression is always better than tension. Upto 4.3X / 2.3X enhancement possible with 2% uniaxial / biaxial compression. Enhancement with strain (specially for Uniaxial) depends highly on the choice of channel direction.